Magnetic Pressure and Shape of Ferrofluid Seals in Cylindrical Structures

Romain Ravaud, Guy Lemarquand, Valérie Lemarquand

Magnetic Pressure and Shape of Ferrofluid Seals in Cylindrical Structures

R. Ravaud, G. Lemarquand, V. Lemarquand

Abstract

This paper presents a three-dimensional analytical model for studying the shape and the pressure of ferrofluid seals in totally ironless structures. This three-dimensional analytical approach is based on the exact calculation of the magnetic field components created by ring permanent magnets whose polarizations are either radial or axial. We assume that the ferromagnetic particles of the ferrofluid are saturated. Moreover, the permanent magnets (Neodymium Iron Boron) used in the considered applications create a magnetic field which is much higher than the magnetic field created by the magnetic particles in the ferrofluid so the latter is neglected. Nevertheless, the static behavior of the ferrofluid seal depends on both the magnetic field produced by the permanent magnets and the saturation magnetization of the ferrofluid particles. Furthermore, the accurate knowledge of the ferrofluid seal shape as well as the magnetic pressure inside the ferrofluid seal is very useful for the design of devices using both permanent magnets and ferrofluid seals. It is emphasized here that our structures are completely ironless and thus, there are no iron-base piston for these structures. Then, this paper makes a review of the main structures using ring permanent magnets and ferrofluid seals. For each ironless structure, the shape and the pressure of the ferrofluid seals are determined.

Index Terms

ferrofluid seals, analytical approach, permanent magnets, magnetic pressure

Manuscript Received January 14, 2009, first revision May 13, second revision June 30, 2009.

The authors are with the Laboratoire d'Acoustique de l'Universite du Maine UMR CNRS 6613, Avenue Olivier Messiaen, 72085 Le Mans Cedex 9, France. Corresponding author guy.lemarquand@ieee.org

I. Introduction

The interest of using ferrofluid in the new technologies increases clearly with the understanding of its chemical and physical properties [1]-[3]. Ferrofluids are in fact a unique class of material that have been discovered in the 1960s. A ferrofluid is a stable colloidal suspension of sub-domain magnetic nano particles in a liquid carrier. These magnetic particles are coated with a stabilizing dispersing agent that prevents generally particle agglomeration. Such a property is very useful because in some applications (as the ones presented in this paper), the magnetic fields used are very intense. Besides, it is noted that we discuss the utility of using intense magnetic fields in this paper. Some industries use ferrofluids for realizing airtightness seals or in audio engineering to decrease the temperature of coils in loudspeakers. As this choice allows us to improve greatly these devices, a care study of the shape of a ferrofluid seal must be carried out because this property is directly linked to its magnetic energy and its mechanical properties. Their properties prove to be useful and efficient in various engineering areas such as damping systems [4], heat transfers, motion control systems, sensors [5][6]. They also have very promising medical applications [7] [8]. However, they are more commonly used in bearings and seals for rotating devices. The pioneering work regarding the ferrofluid lubrication was done by Tarapov [9]. Indeed, he considered a plain journal bearing lubricated by ferrofluid and submitted to a non-uniform magnetic field. Since then, numerous studies in the field of ferrofluid dynamic bearings have been carried out. Both static and dynamic characteristics of these bearings have been studied theoretically [10]-[17]. Moreover, recent trends in the ferrofluid lubrication applications are described and discussed [18]-[24]. Ferrofluids are also used in electrodynamic loudspeakers in which they fulfill several functions: they ensure the airtightness, they play a heat transfer part and they work as a radial bearing. Furthermore, a ferrofluid seal can replace the loudspeaker suspension and leads to a better linearity of the cone movement [25]-[29].

This paper presents a three-dimensional analytical model for studying the shape and the static pressure of ferrofluid seals submitted to intense magnetic fields produced by ironless structures. We use the static magnetic pressure for studying the shape of the ferrofluid seals. Our three-dimensional analytical approach is based on the exact calculation of the magnetic field components created by ring permanent magnets whose polarizations are either radial or axial. Moreover, the approach taken is based on the coulombian

model of permanent magnets. Consequently, it gives a great flexibility for the review of the different structures studied in this paper.

In addition, it must be emphasized here that our experimental conditions in which the ferrofluid is used differ from the other experiments proposed by the authors. Indeed, our applications (ironless loudspeakers, bearings) require very high magnetic fields. Consequently, we think that the most important parameter representing the pressure in the ferrofluid seal must be determined carefully. This term is often simplified in many studies because it is difficult to determine. However, this term is not only the most important parameter that must be determined carefully but this is also probably the only term that allows us to study the ferrofluid seal shape. The gravitational energy or the surface tension energy do not influence a ferrofluid seal shape used in these conditions. This is why we think that it is more useful to obtain an exact three-dimensional analytical expression of the magnetic pressure by only considering the preponderant term in the equation of equilibrium in the ferrofluid seal rather than using several simplifying terms whose influence is questionable in our applications.

As the ferrofluid considered in this paper (Ferrotec APG05) has a saturation magnetization of at least 32 kA/ m and the magnetic field is greater than $400kA/m$, the value of this pressure is higher than 12800 $\mathrm{N/m^2}$. On the other hand, the surface tension exists. But when the values of both the surface tension coefficient, A, (A equals $0.0256kg/s^2$ for the used ferrofluids) and the radius of curvature are considered, the effect of the surface tension can be omitted: this latter does not deform the free boundary surface.

II. Three-Dimensional Analytical Model

First, we present the calculation tools to study the different configurations using one or several ring permanent magnets. As the goal of this paper is to determine the shape of the ferrofluid seals for different magnet configurations, the magnetic field created by the magnets must be calculated. Then, the way of obtaining the seal shape is discussed.

It is emphasized here that we do not use a two-dimensional model for calculating the magnetic field created by these arc-shaped permanent magnets because such an approach is not accurate in the near-field [30]. This is the reason why we use only a three-dimensional approach.

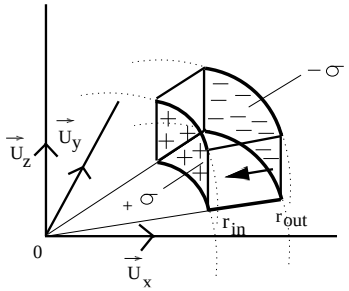

Fig. 1. Arc-shaped permanent magnet whose polarization is radial: the inner curved surface is charged with the magnetic pole surface density $+\sigma^*$ and the outer curved surface is charged with the magnetic pole surface density $-\sigma^*$, the inner radius is r_{in}, the outer one is r_{out}

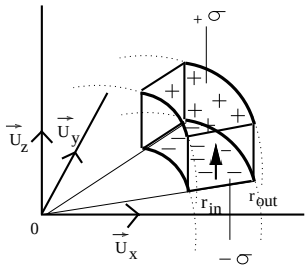

Fig. 2. Arc-shaped permanent magnet whose polarization is axial: the upper surface is charged with the magnetic pole surface density $+\sigma^*$ and the lower surface is charged with the magnetic pole surface density $-\sigma^*$, the inner radius is r_{in}, the outer one is r_{out}

A. Magnetic field created by the ring magnets

The magnetic field created by the ring magnets is determined by using the coulombian model. The magnets are assumed perfect (flawless) with a perfectly uniform magnetization. Consequently, each permanent magnet is represented by two charged surfaces. In the case of a permanent magnet whose polarization is radial, the magnetic poles are located on both curved surfaces of the ring and the magnetic pole surface density is denoted σ^* (Fig. 1). The rings are assumed radially thin enough to neglect the magnetic pole volume density related to the magnetization divergence. In the case of a permanent magnet whose polarization is axial, the magnetic pole surface density σ^* is located on the upper and lower faces of the ring (Fig. 2). The magnetic field components have been entirely determined in previous papers [30][31]. Since the azimuthal component equals zero because of the cylindrical symmetry [32], only two components must be calculated. Therefore, the magnetic field depends on both radius r and altitude z.

B. Potential energy and magnetic pressure of the ferrofluid seal

The potential energy of the ferrofluid is very important parameter for the study of ferrofluid seals. Its calculation requires several assumptions, generally admitted by the authors. First, the ferromagnetic particles of the ferrofluid are assumed to be small saturated spheres which can be freely oriented in all the directions of space. Thus, all the particles of the saturated ferrofluid are aligned with the permanent magnet orienting field. In addition, when submitted to these intense magnetic fields, the ferrofluid does not modify the field created by the permanent magnets and the field created by the ferrofluid itself is omitted. Furthermore, the aggregation in chains of the ferrofluid particles is omitted [33]. It is noted that, when the device is at laboratory temperature and at rest, the aggregation phenomenon is observed. In short, the magnetic pressure is expressed as follows:

$$p_m(r,z) = \mu_0 \mathbf{M_s}.\mathbf{H}(r,z) = \mu_0 M_s \sqrt{H_r(r,z)^2 + H_z(r,z)^2} \tag{1}$$

where both magnetic field components $H_r(r,z)$ and $H_z(r,z)$ are analytically calculated [30]. Thus, the potential energy of the ferrofluid seal, E_m, can be deducted :

$$E_m = -\int\int\int_{(\Omega)} \mathbf{H}(r,z).(\mu_0 \mathbf{M}) dV = -\int\int\int_{(\Omega)} p_m(r,z) dV \tag{2}$$

where (Ω) is the ferrofluid seal volume. As a remark, the magnetic pressure is given in N/m^2 and the potential energy in J. The analytical expression of the magnetic pressure depends on the number of ring permanent magnets used in the ironless structure. For example, if we consider a structure made of two ring permanent magnets radially magnetized, with opposite magnetizations, the magnetic pressure $p_m(r,z)$ inside the ferrofluid seal is given by (3).

$$p_m(r,z) = \mu_0 M_s \sqrt{H_{r,2}(r,z)^2 + H_{z,2}(r,z)^2} \tag{3}$$

where M_s is the intensity of magnetization of a magnetic particle. The radial component $H_{r,2}(r,z)$ of the magnetic field created by the two permanent magnets is defined by (4).

$$H_{r,2}(r,z) = \frac{\sigma^*}{2\pi\mu_0} \left(\varsigma(u_1) - \varsigma(u_2)\right) \tag{4}$$

with

$$
\begin{aligned}
\varsigma(u) \quad = \quad & \left(\frac{2i(1+u)\sqrt{\frac{d(-1+u)}{c+e_1+du}}\left(-(a_1 d+b_1(c+e_1))\right) F^*\left[i\sinh^{-1}[\frac{\sqrt{-c+d-e_1}}{\sqrt{c+e_1+du}}],\frac{c+d+e_1}{c-d+e_1}\right]}{d\sqrt{-c+d-e_1}e_1\sqrt{\frac{d(1+u)}{c+e_1+du}}\sqrt{1-u^2}} \right) \\
& + \left(\frac{2i(1+u)\sqrt{\frac{d(-1+u)}{c+e_1+du}}(b_1 c-a_1 d)\Pi^*\left[\frac{e_1}{c-d+e_1},i\sinh^{-1}[\frac{\sqrt{-c+d+e_1}}{c+e_1+du}],\frac{c+d+e_1}{c-d+e_1}\right]}{d\sqrt{-c+d-e_1}e_1\sqrt{\frac{d(1+u)}{c+e_1+du}}\sqrt{1-u^2}} \right) \\
& + \left(\frac{2i(1+u)\sqrt{\frac{d(-1+u_1)}{c+e_2+du_1}}\left(-(a_2 d+b_2(c+e_2))\right) F^*\left[i\sinh^{-1}[\frac{\sqrt{-c+d-e_2}}{\sqrt{c+e_2+du}}],\frac{c+d+e_2}{c-d+e_2}\right]}{d\sqrt{-c+d-e_2}e_2\sqrt{\frac{d(1+u)}{c+e_2+du}}\sqrt{1-u^2}} \right) \\
& + \left(\frac{2i(1+u)\sqrt{\frac{d(-1+u)}{c+e_2+du}}(b_2 c-a_2 d)\Pi^*\left[\frac{e_2}{c-d+e_2},i\sinh^{-1}[\frac{\sqrt{-c+d+e_2}}{c+e_1+du}],\frac{c+d+e_2}{c-d+e_2}\right]}{d\sqrt{-c+d-e_2}e_2\sqrt{\frac{d(1+u)}{c+e_2+du}}\sqrt{1-u^2}} \right) \\
& - \left(\frac{2i(1+u)\sqrt{\frac{d(-1+u)}{e_3+du}}\left((a_3 d-b_3 e_3)\right) F^*\left[i\sinh^{-1}[\frac{\sqrt{-d-e_3}}{\sqrt{e_3+du}}],\frac{-d-e_3}{d+e_3}\right]}{d\sqrt{-d-e_3}(-c+e_3)\sqrt{\frac{d(1+u)}{e_3+du}}\sqrt{1-u^2}} \right) \\
& - \left(\frac{2i(1+u)\sqrt{\frac{d(-1+u)}{e_1+du}}(b_3 c-a_3 d)\Pi^*\left[\frac{-c+e_3}{d+e_3},i\sinh^{-1}[\frac{\sqrt{-d+e_3}}{e_3+du}],\frac{-d+e_3}{d+e_3}\right]}{d\sqrt{-d-e_3}(-c+e_3)\sqrt{\frac{d(1+u)}{e_3+du}}\sqrt{1-u^2}} \right) \\
& - \left(\frac{2i(1+u)\sqrt{\frac{d(-1+u)}{e_4+du}}\left(a_4 d-b_4 e_4\right) F^*\left[i\sinh^{-1}[\frac{\sqrt{-d-e_4}}{\sqrt{e_4+du}}],\frac{-d+e_4}{d+e_4}\right]}{d\sqrt{-d-e_4}(c+e_4)\sqrt{\frac{d(1+u)}{e_4+du}}\sqrt{1-u^2}} \right) \\
& - \left(\frac{2i(1+u)\sqrt{\frac{d(-1+u)}{e_4+du}}(b_4 c-a_4 d)\Pi^*\left[\frac{-c+e_4}{d+e_4},i\sinh^{-1}[\frac{\sqrt{-d-e_4}}{e_4+du}],\frac{-d+e_4}{d+e_4}\right]}{d\sqrt{-d-e_4}(-c+e_4)\sqrt{\frac{d(1+u)}{e_4+du}}\sqrt{1-u^2}} \right)
\end{aligned}
\tag{5}
$$

The axial component of the magnetic field created by the two ring permanent magnets is given by (6).

$$
\begin{aligned}
H_{z,2}(r,z) \quad = \quad & \frac{\sigma^*}{\pi\mu_0}\left(-r_{in}\frac{K^*\left[-\frac{4rr_{in}}{(r-r_{in})^2+z^2}\right]}{\sqrt{(r-r_{in})^2+z^2}} + r_{in}\frac{K^*\left[-\frac{4rr_{in}}{(r-r_{in})^2+(z-h)^2}\right]}{\sqrt{(r-r_{in})^2+(z-h)^2}} \right) \\
& - \frac{\sigma^*}{\pi\mu_0}\left(r_{in}\frac{K^*\left[\frac{4rr_{in}}{(r-r_{in})^2+z^2}\right]}{\sqrt{(r-r_{in})^2+z^2}} - r_{in}\frac{K^*\left[\frac{4rr_{in}}{(r-r_{in})^2+(z+h)^2}\right]}{\sqrt{(r-r_{in})^2+(z+h)^2}} \right)
\end{aligned}
\tag{6}
$$

Parameters	
a_1	$r_{in}rz$
b_1	$\text{-}r_{in}^2 z$
c	$r^2 + r_{in}^2$
d	$-2rr_{in}$
e_1	z^2
a_2	$-r_{in}r(z-h)$
b_2	$r_{in}^2(z-h)$
e_2	$(z-h)^2$
a_3	$r_{in}rz$
b_3	$-r_{in}^2 z$
e_3	$r^2 + r_{in}^2 + z^2$
a_4	$r_{in}r(-z-h)$
b_4	$-r_{in}^2(-z-h)$
e_4	$r^2 + r_{in}^2 + (z+h)^2$

TABLE I

DEFINITION OF THE PARAMETERS USED IN (5)

where $K^*[m]$ is given in terms of the incomplete elliptic integral of the first kind by (7)

$$K^*[m] = F^*[\frac{\pi}{2}, m] \tag{7}$$

$F^*[\phi, m]$ is given in terms of the elliptic integral of the first kind by (8):

$$F^*[\phi, m] = \int_{\theta=0}^{\theta=\phi} \frac{1}{\sqrt{1 - m\sin(\theta)^2}} d\theta \tag{8}$$

$\Pi^*[n, \phi, m]$ is given in terms of the incomplete elliptic integral of the third kind by (9)

$$\Pi^*[n, \phi, m] = \int_0^{\phi} \frac{1}{(1 - n\sin(\theta)^2)\sqrt{1 - m\sin(\theta)^2}} d\theta \tag{9}$$

The parameters used in (5) are defined in Table II-B. Moreover, when we input (4) in Mathematica, we have to take the real part of $H_r(r, z)$ because of the noise calculus. What's more, the parameter i used in (5) is the imaginary number $(i^2 = -1)$.

C. Parameters used for describing the ironless structures

The further calculations are presented for magnets with 1T remanent magnetization in order to normalize the results. In fact, the magnets used in the prototypes are Neodymium Iron Boron ones for which the remanent magnetization can reach 1.5T. Furthermore, the interesting regions of space are the ones where the ferrofluid goes. With these 1T normalized magnets and for the proposed configurations, the magnetic field intensity there is greater than 400 kA/m. Of course, all the field values are proportional to remanent magnetization value. Then, we use commercial ferrofluids, either from the company Ferrotec or Ferrolabs . Such ferrofluids have a saturation magnetization, M_s, smaller than 32 kA/m and a particle concentration below 5,5 %. It is to be noted that for bearing or loudspeaker applications, a great bearing effect is seeked which requires high saturation magnetizations. Therefore, the magnetic field, H, created by the permanent magnets is far higher than the ferrofluid critical field [34]. So, the ferrofluid is totally saturated and its magnetization is denoted M_s.

Color plots of the magnetic pressure will be done in the further sections in order to visualize the characteristics of the studied configurations. The warmest color (red) is used for the regions of space where the magnetic pressure is the greatest and the coldest color (blue) for the ones where the magnetic pressure is the smallest. Moreover, the same color corresponds to the same value throughout this paper: the corresponding scale is given in Table II in which the magnetic pressure and the related magnetic field values are given.

III. Shape of the ferrofluid seal in various magnetic fields

A. Description of the generic structure

Figure 3 shows the generic structure of all the devices studied. They consist of three outer stacked rings, of an inner non-magnetic piston and of ferrofluid seals. The piston is radially centered with the rings. The rings' inner radius, r_{in}, equals 25 mm and their outer radius, r_{out}, equals 28 mm. The rings can be either made out of permanent magnet -as here the middle ring- or out of non-magnetic material -like the upper and lower rings-. For each configuration, the ferrofluid seals are located in the air gap between the piston and the rings; their number, their position as well as the magnetization direction of

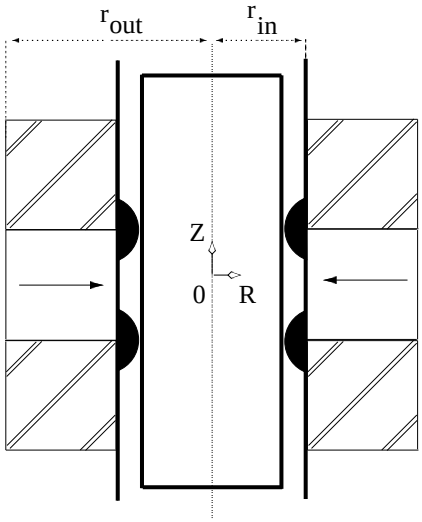

Fig. 3. Device structure: three outer rings (permanent magnet or non-magnetic) radially centered with an inner non-magnetic piston and ferrofluid seals in the air gap between the rings and the piston. $r_{in} = 25mm$, $r_{out} = 28mm$.

the ring magnets will be discussed.

For each configuration, we have also represented the radial component of the magnetic field created by the ring permanent magnets: indeed, this parameter can also be optimized by changing the ring dimensions in electric machines.

It is assumed throughout this paper that the forming shapes of ferrofluid are considered to be proportional to the magnetic pressure. Such an assumption is possible because the magnetic field produced by the ring permanent magnets is very high.

The coordinate system (0,$\vec{u}_r, \vec{u}_\theta, \vec{u}_z$) is placed into the centre of the magnetic system in Figs 6 and 7 and is axially moved off the centre in Figs 4, 5, 8, 9, 10 and 11. In addition, the radial scale of the permanent magnets has been divided by 2 in these figures.

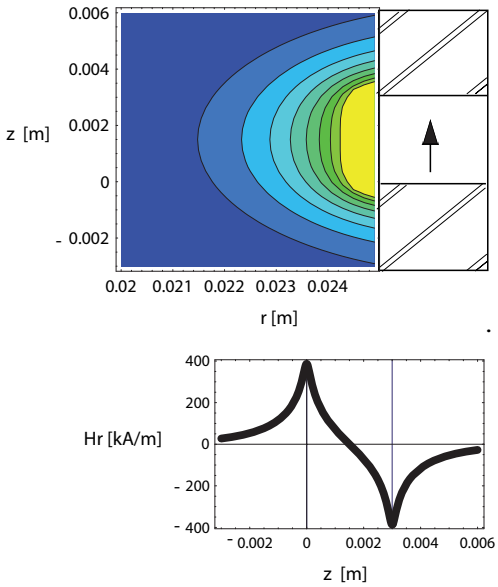

Fig. 4. Right: upper and lower non-magnetic rings, a middle ring permanent magnet axially magnetized. Left: magnetic pressure in front of the rings. Bottom: magnetic field radial component at a 0.1 mm distance from the rings, along the Z axis.

B. Structures using one ring magnet

The first structure considered corresponds exactly to the configuration shown in Fig.3. All the rings have the same square cross-section whose side equals 3 mm. The middle ring is a radially magnetized permanent magnet and the upper and lower rings are non-magnetic. The magnetic field created by the magnet in the air gap is calculated at a distance in length from the rings and along the Z axis which equals 0.1 mm. Moreover, its radial component H_r shown in Fig.4 is quite uniform in front of the magnet. Two field gradients exist in front of the edges of the magnet. We can point out that the magnetic pressure calculated in the air gap between the rings and the piston is plotted on Fig.4 as well. The ferrofluid seeks the regions of both intense field gradient and high magnetic energy. The color plot shows that, for seals thicker than 0.5 mm, the seal expands along the whole magnet height. A smaller amount of ferrofluid would give two separate seals, but they would be too thin to have interesting mechanical properties. This result is linked to the magnet square section: were the magnet higher along Z, two separate seals would appear. It can be noted that this structure is the simplest one which can be used in electrodynamic loudspeakers.

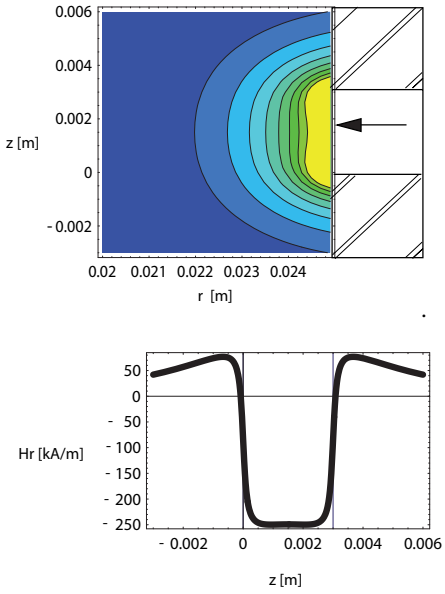

Fig. 5. Right: upper and lower non-magnetic rings, a middle ring permanent magnet radially magnetized. Left: magnetic pressure in front of the rings. Bottom: magnetic field radial component at a 0.1 mm distance from the rings, along the Z axis.

The second structure differs from the first one only in the magnetization direction which becomes axial. Figure 5 shows the structure, the calculated radial field component and the corresponding magnetic pressure. The radial component of the magnetic field is no longer uniform in front of the magnet; it shows instead a rather large gradient all over the magnet length and the non-magnetic rings. Nevertheless, the magnetic pressure deserves the same comments as in the first structure and is somewhat similar to the previous one. However, it is obvious that it differs in form from one structure to the other.

C. Structures using two ring magnets

The structures studied here derive from the preceding ones by stacking a second permanent magnet ring directly on the first one. Both ring magnets have the same dimensions and opposed magnetization directions. The radial field component and the magnetic pressure are shown in Fig. 7 when the ring magnets are radially magnetized and in Fig. 6 when the ring magnets are axially magnetized. The magnetic field

in both cases results from the superposition of the single magnet fields. As a consequence, each radial magnet creates a region of uniform field in front of itself and the field directions are opposite. The field intensity in each uniform region is higher than in the single magnet structure because the leakage is decreased. In effect, three field gradients exist, and the one that appears in front of the magnets' interface is twice as high as those at the edges. From the gradient point of view, Fig. 7 can be compared with Fig. 5, and the former will prove more useful because the gradient is steeper. The axial double structure creates progressive field gradients with no peculiar interest. By contrast, the radial double structure is used to design two-coil loudspeakers. The repartition of the magnetic energy density in the structure using two ring magnets does not derive from the superposition of the ones in the structures using one ring magnet. The main reason is due to the expression of the energy which depends on the square of the field. Both repartitions for radial and axial magnets seem alike at first sight, but the radial structure is in fact "more energetic" and the magnetic energy in it decreases slower at an increasing distance from the magnets. Nevertheless, the maximum energy density is in front of the magnets' interface and the ferrofluid seal will be located there. We can point out that the axial length of the seal in structures using one magnet is smaller than the one in structures using two ring magnets. Furthermore, its energy density is approximately doubled for the radial magnets.

D. Structures using three ring magnets

All the structures considered now consist of three stacked ring permanent magnets whose magnetization directions undergo a 90 degrees rotation from one magnet to the neighboring one. Such configurations with a magnetization progressive rotation are related to Halbach cylinders [35] and to their applications in the design of electrical motors [36], sensors [37][38] or of passive magnetic bearings [39]. Contrary to electrical machines, the presented structures do not have a periodical magnet pattern.

Figure 8 shows the field radial component and the magnetic pressure for an assembly of a radially magnetized middle ring and two axially magnetized upper and lower rings. Moreover, the axial magnets have opposed magnetization directions. In Fig. 9, the middle ring is axially magnetized, both other rings are radially magnetized with opposed directions.

The energy density color plots show that two ferrofluid seals form in front of the magnets' interfaces

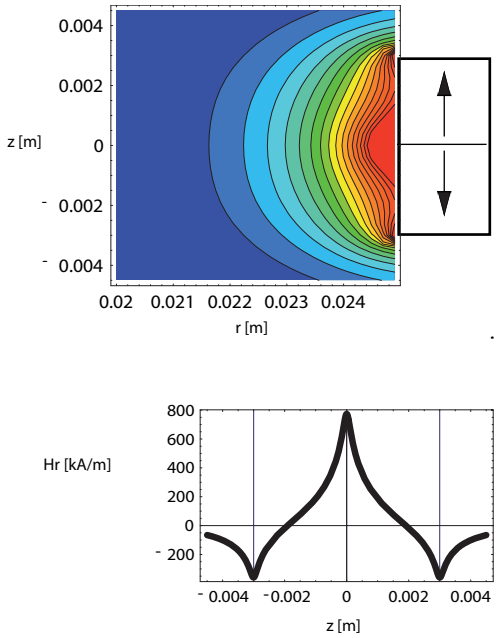

Fig. 6. Right: Two ring permanent magnets with opposed axial magnetization. Left: magnetic pressure in front of the rings. Bottom: magnetic field radial component at a 0.1 mm distance from the rings, along the Z axis.

and that those seals have a great magnetic energy. Consequently, they own good mechanical properties (great radial stiffness for example). The seals are rather similar in both structures. However, the magnetic field radial component shown in Fig. 8 is fairly uniform in the area in front of the middle magnet while it varies with no particularly interesting properties in Fig. 9. Therefore, the structure with the radial middle magnet is the useful one, especially for the loudspeaker design, and the field uniformity zone may be optimized.

The axial height of the middle magnet can be varied regarding the axial height of the upper and lower magnets. For example, the middle magnet is twice as high as each other magnet in Fig. 10 and half as small in Fig. 11. As a result, the length of the field uniformity area follows closely the middle magnet height. If the latter increases, the former increases too. We can say that the ratio middle of the magnet height over the upper and lower magnet height is important as well. Indeed, if it increases, the field uniformity region grows but the field intensity decreases, and inversely. It also influences the repartition

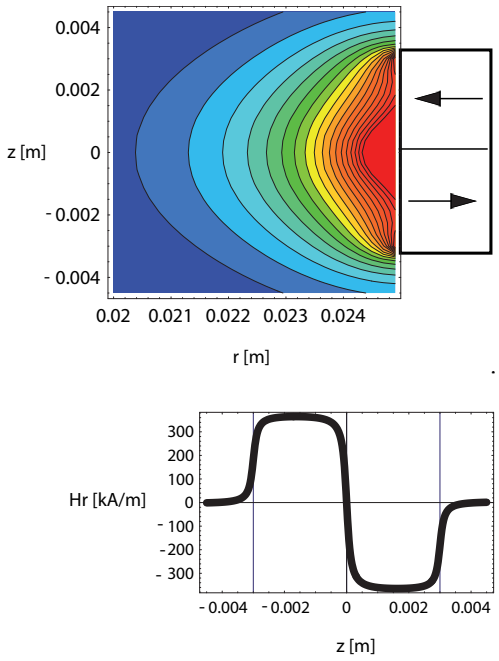

Fig. 7. Right: Two ring permanent magnets with opposed radial magnetization. Left: magnetic pressure in front of the rings. Bottom: magnetic field radial component at a 0.1 mm distance from the rings, along the Z axis.

of the magnetic pressure. Indeed, when the upper and lower magnets become too small, the ferrofluid can expand over their whole axial length and the seals can become fairly voluminous, depending on the ferrofluid available quantity. The field gradients are steep and the seal magnetic energy is quite high. Consequently, the seals are well-fixed to the structure and have high mechanical performances. Inversely, when the middle magnet becomes too small, both seals gather to form a single one which expands over the whole height of the middle magnet. The energy in the seal is still high for radial thickness smaller than the ones presented in the previous case.

E. Discussion

So far, different magnet assemblies have been presented. Each assembly creates magnetic fields and magnetic field gradients so as to trap and fix ferrofluid to make seals. Their characteristics will be discussed and compared now.

The structures considered are either very simple or more complex. The complexity can be characterized

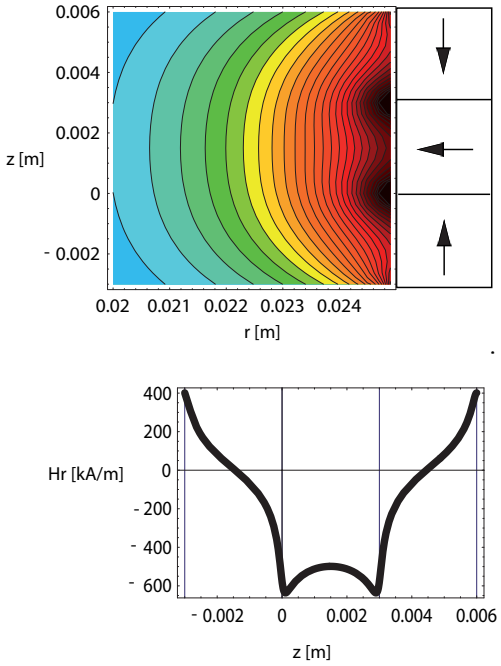

Fig. 8. Right: axially magnetized upper and lower rings, radially magnetized middle ring. Left: magnetic pressure in front of the rings. Bottom: magnetic field radial component at a 0.1 mm distance from the rings, along the Z axis.

by the number of separate parts necessary to build devices. We can say that from this point of view, the single magnet structures are the simplest ones. The complexity also lies in the magnets' magnetization direction. Indeed, an axial magnetization is easy to achieve for ring magnets whereas a radial one is technically more difficult. Thereby, ring magnets whose polarization is radial are more expensive than the ones whose polarization is axial. Nevertheless, some magnet manufacturers begin to deal with radial magnetization and to sell such products.

The utility of a structure depends on the intended applications. For example, a device can be designed solely to make ferrofluid seals with good mechanical properties. It can also be designed to create a radial magnetic field or to enable a ferrofluid seal to form as it is required in loudspeakers.

A high magnetic field gradient and a high magnetic pressure are required to achieve robust seals. From the preceding sections, we deduce that multi-magnet structures are more efficient than single magnet

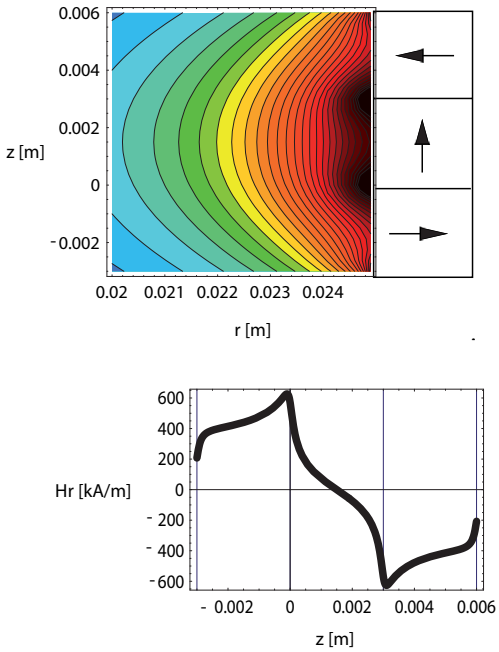

Fig. 9. Right: radially magnetized upper and lower rings, axially magnetized middle ring. Left: magnetic pressure in front of the rings. Bottom: magnetic field radial component at a 0.1 mm distance from the rings, along the Z axis.

structures in creating high field gradients. Furthermore, the magnetic pressure is higher in the air gap near the magnets.

It can be emphasized here that the shape of the ferrofluid seal in the device depends on both the magnetic pressure and the ferrofluid volume. It can be noted that this latter one is related to the air gap size. The air gap exists because the inner part has to move, in rotation or in translation, inside the outer part without rubbing against it. The air gap size depends on mechanical considerations, such as the practical machining and the related possible tolerances. The color plots show clearly that the theoretical size of the air gap which allows an efficient ferrofluid seal depends on the magnetic structure dimensions.

For example, the structures shown in Fig. 11 or in Fig. 8 lead to seals thinner than the ones shown in Fig. 7 because the region of high magnetic pressure is radially thinner.

Ferrofluid seals are robust when their capacity is high; this means that they can resist to quite high axial pressures because they exert themselves an opposing force. We can say that this force is related to

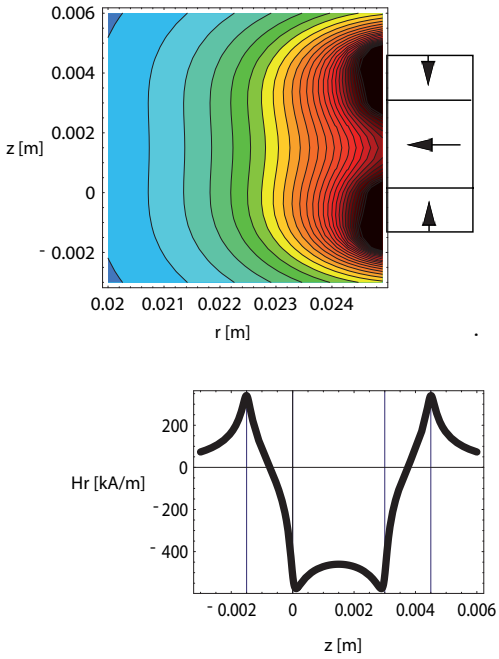

Fig. 10. Right: axially magnetized upper and lower rings, radially magnetized middle ring, each axial magnet is half as small as the radial one. Left: magnetic pressure in front of the rings. Bottom: magnetic field radial component at a 0.1 mm distance from the rings, along the Z axis.

the energy variation of the ferrofluid seal. The higher the energy varies with the axial displacement, the more important the force is.

Moreover, a great force is attained with thin seals whose energy is high and varies extremely with axial displacements. Therefore, the smaller the air gap is, the more favorable the mechanical structure to build ferrofluid seals is.

The color plots can help optimizing both the number and the shape of ferrofluid seals for given ferrofluid volumes.

For example, the plots shown in Figs. 10 and 11 point out that two seals appear in these three magnet structures for a small volume of ferrofluid. Moreover, they show that the increase in the ferrofluid volume results in the growth of the seals which eventually join and can form a single big one.

The color plots can also be considered as tools to determine the adequate quantity of ferrofluid which will confer the intended mechanical properties on the seals. Furthermore, this study shows that some

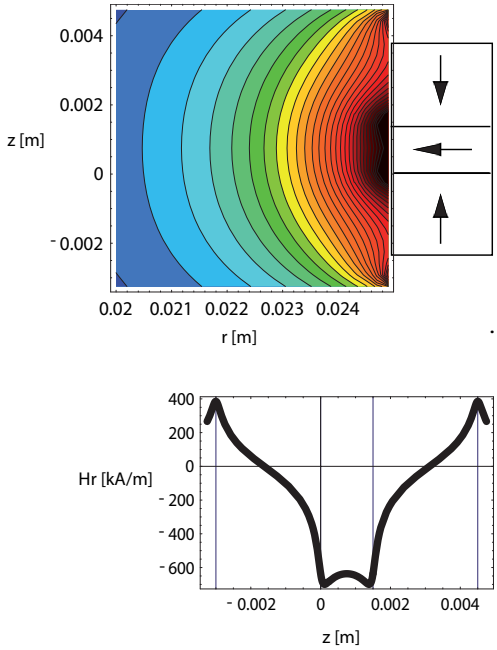

Fig. 11. Right: axially magnetized upper and lower rings, radially magnetized middle ring, each axial magnet is twice as high as the radial one. Left: magnetic pressure in front of the rings. Bottom: magnetic field radial component at a 0.1 mm distance from the rings, along the Z axis.

structures have greater performances than others for given magnet and ferrofluid volumes.

The requirements for the loudspeaker applications are different. Indeed, the magnetic structure is expected to fulfill several purposes, namely the creation of a radial uniform magnetic field as well as the creation of field gradients. Besides, a loudspeaker coil moves thanks to the magnetic field. The linearity performances are related to the field uniformity and the efficiency is proportional to the field level. Furthermore, the ferrofluid seal is used to ensure the airtightness, to transfer the heat from the moving part to the steady one, to work as a radial bearing and to replace the loudspeaker suspension. Thereby, it contributes to the improvement of the loudspeaker linearity. The air gaps in loudspeakers are generally 0.1 to 0.5 mm wide: this explains why the presented magnetic field calculations have been carried out along a path at a distance in length which equals 0.1 mm from the ring magnets. Thinner air gaps would be more advantageous for ferrofluid seals but are not technically possible because of the machining tolerances or the recognition of the moving part thermal dilation. Therefore, the structures

shown in Figs. 3, 7 and 10 are the ones that are the more useful for loudspeakers. The three magnet structures are the more complex, but they offer the possibility of a multi-criteria optimization. We can say that this optimization is enabled and simplified by the analytical formulations of both the magnetic field and the magnetic energy density. Eventually, such structures show very good performances.

IV. Conclusion

This paper has presented a three-dimensional analytical model for studying the shape of the static pressure of ferrofluid seals subject to intense magnetic fields produced by permanent magnet ironless structures. Our analytical approach has been applied to well-known structures composed of one, two or three stacked ring permanent magnets whose polarization is either radial or axial. Our analytical appraoch allows us to predict easily the shape and the pressure of ferrofluid seals. Then, we have discussed the interest of using simple or complex structures with ferrofluid seals. The single magnet structures are the simplest ones but the less efficient. The use of several magnets enhances both magnetic and mechanical properties: when the created magnetic field is doubled, the magnetic energy is quadrupled. Furthermore, three magnet structures enable to create one or two seals which have a high energy. The structures can also create a high uniform magnetic field over defined regions as well as efficient ferrofluid seals: this is useful for loudspeaker applications. The results obtained can be used for the design of cylindrical structures using both ring permanent magnets and ferrofluid seals.

References

[1] H. S. Choi, Y. S. Kim, K. T. Kim, and I. H. Park, “Simulation of hydrostatical equilibrium of ferrofluid subject to magneto-static field,” *IEEE Trans. Magn.*, vol. 44, no. 6, pp. 818–821, 2008.

[2] K. Raj, V. Moskowitz, and R. Casciari, “Advances in ferrofluid in ferrofluid technology,” *Journal of Magnetism and Magnetic Materials*, vol. 149, pp. 174–180, 1995.

[3] Y. L. Raikher, V. I. Stepanov, J. C. Bacri, and R. Perzynski, “Orientational dynamics in magnetic fluids under strong coupling of external and internal relaxations,” *Journal of Magnetism and Magnetic Materials*, vol. 289, pp. 222–225, 2005.

[4] J. Bajkowski, J. Nachman, M. Shillor, and M. Sofonea, “A model for a magnetorheological damper,” *Mathematical and computer modelling*, vol. 48, pp. 56–68, 2008.

[5] R. E. Rosensweig, *Ferrohydrodynamics*. Dover, 1997.

[6] O. Doutres, N. Dauchez, J. M. Genevaux, and G. Lemarquand, “On the use of a loudspeaker for measuring the viscoelastic properties of sound absorbing materials,” *Journal of the Acoustical Society of America Express Letters*, vol. 124, no. 6, pp. EL335–EL340, 2008.

[7] X. Li, K. Yao, and Z. Liu, "Cfd study on the magnetic fluid delivering in the vessel in high-gradient magnetic fields," *Journal of Magnetism and Magnetic Materials*, vol. 320, pp. 1753–1758, 2008.

[8] G. S. Park and K. Seo, "New design of the magnetic fluid linear pump to reduce the discontinuities of the pumping forces," *IEEE Trans. Magn.*, vol. 40, pp. 916–919, 2004.

[9] I. Tarapov, "Movement of a magnetizable fluid in lubricating layer of a cylindrical bearing," *Magnetohydrodynamics*, vol. 8, no. 4, pp. 444–448, 1972.

[10] J. Walker and J. Backmaster, "Ferrohydrodynamics thrust bearings," *Int. J. Eng. Sci.*, vol. 17, pp. 1171–1182, 1979.

[11] N. Tiperi, "Overall characteristics of bearings lubricated ferrofluids," *ASME J. Lubr. Technol.*, vol. 105, pp. 466–475, 1983.

[12] S. Miyake and S. Takahashi, "Sliding bearing lubricated with ferromagnetic fluid," *ASLE Trans.*, vol. 28, pp. 461–466, 1985.

[13] H. Chang, C. Chi, and P. Zhao, "A theoretical and experimental study of ferrofluid lubricated four-pocket journal bearing," *Journal of Magnetism and Magnetic Materials*, vol. 65, pp. 372–374, 1987.

[14] Y. Zhang, "Static characteristics of magnetized journal bearing lubricated with ferrofluids," *ASME J. Tribol.*, vol. 113, pp. 533–538, 1991.

[15] T. Osman, G. Nada, and Z. Safar, "Static and dynamic characteristics of magnetized journal bearings lubricated with ferrofluid," *Tribology International*, vol. 34, pp. 369–380, 2001.

[16] R. C. Shah and M. Bhat, "Anisotropic permeable porous facing abd slip velocity squeeze film in axially undefined journal bearing with ferrofluid lubricant," *Journal of Magnetism and Magnetic Materials*, vol. 279, pp. 224–230, 2004.

[17] F. Cunha and H. Couto, "A new boundary integral formulation to describe three-dimensional motions of interfaces between magnetic fluids," *Applied mathematics and computation*, vol. 199, pp. 70–83, 2008.

[18] R. C. Shah and M. Bhat, "Ferrofluid squeeze film in a long bearing," *Tribology International*, vol. 37, pp. 441–446, 2004.

[19] S. Chen, Q. Zhang, H. Chong, T. Komatsu, and C. Kang, "Some design and prototyping issues on a 20 krpm hdd spindle motor with a ferro-fluid bearing system," *IEEE Trans. Magn.*, vol. 37, no. 2, pp. 805–809, 2001.

[20] Q. Zhang, S. Chen, S. Winoto, and E. Ong, "Design of high-speed magnetic fluid bearing spindle motor," *IEEE Trans. Magn.*, vol. 37, no. 4, pp. 2647–2650, 2001.

[21] P. Kuzhir, "Free boundary of lubricant film in ferrofluid journal bearings," *Tribology International*, vol. 41, pp. 256–268, 2008.

[22] M. Miwa, H. Harita, T. Nishigami, R. Kaneko, and H. Unozawa, "Frequency characteristics of stiffness and damping effect of a ferrofluid bearing," *Tribology Letter*, vol. 15, no. 2, pp. 97–105, 2003.

[23] W. Ochonski, "The attraction of ferrofluid bearings," *Mach. Des.*, vol. 77, no. 21, pp. 96–102, 2005.

[24] Z. Meng and Z. Jibin, "An analysis on the magnetic fluid seal capacity," *Journal of Magnetism and Magnetic Materials*, vol. 303, pp. e428–e431, 2006.

[25] R. E. Rosensweig, Y. Hirota, S. Tsuda, and K. Raj, "Study of audio speakers containing ferrofluid," *J. Phys. : Condens. Matter*, vol. 20, 2008.

[26] G. Lemarquand, "Ironless loudspeakers," *IEEE Trans. Magn.*, vol. 43, no. 8, pp. 3371–3374, 2007.

[27] R. Ravaud and G. Lemarquand, "Modelling an ironless loudspeaker by using three-dimensional analytical approaches," *Progress in Electromagnetics Research, PIER 91*, pp. 53–68, 2009.

[28] R. Ravaud, G. Lemarquand, V. Lemarquand, and C. Depollier, "Ironless loudspeakers with ferrofluid seals," *Archives of Acoustics*, vol. 33, no. 4, pp. 3–10, 2008.

[29] R. Ravaud and G. Lemarquand, “Mechanical properties of a ferrofluid seal: three-dimensional analytical study based on the coulombian model,” *Progress in Electromagnetics research B*, vol. 13, pp. 385–407, 2009.

[30] R. Ravaud, G. Lemarquand, V. Lemarquand, and C. Depollier, “Analytical calculation of the magnetic field created by permanent-magnet rings,” *IEEE Trans. Magn.*, vol. 44, no. 8, pp. 1982–1989, 2008.

[31] R. Ravaud, G. Lemarquand, V. Lemarquand, and C. Depollier, “Discussion about the analytical calculation of the magnetic field created by permanent magnets.,” *Progress in Electromagnetics Research B*, vol. 11, pp. 281–297, 2009.

[32] R. Ravaud, G. Lemarquand, V. Lemarquand, and C. Depollier, “The three exact components of the magnetic field created by a radially magnetized tile permanent magnet.,” *Progress in Electromagnetics Research, PIER 88*, pp. 307–319, 2008.

[33] A. Ivanov, S. Kantorovich, V. Mendelev, and E. Pyanzina, “Ferrofluid aggregation in chains under the influence of a magnetic field,” *Journal of Magnetism and Magnetic Materials*, vol. 300, pp. e206–e209, 2006.

[34] G. Matthies and U. Tobiska, “Numerical simulation of normal-field instability in the static and dynamic case,” *Journal of Magnetism and Magnetic Materials*, vol. 289, pp. 436–439, 2005.

[35] K. Halbach, “Design of permanent multiple magnets with oriented rec material,” *Nucl. Inst. Meth.*, vol. 169, pp. 1–10, 1980.

[36] M. Marinescu and N. Marinescu, “Compensation of anisotropy effects in flux-confining permanent-magnet structures,” *IEEE Trans. Magn.*, vol. 25, no. 5, pp. 3899–3901, 1989.

[37] G. Lemarquand and V. Lemarquand, “Annular magnet position sensor,” *IEEE. Trans. Magn.*, vol. 26, no. 5, pp. 2041–2043, 1990.

[38] C. Blache and G. Lemarquand, “New structures for linear displacement sensor with hight magnetic field gradient,” *IEEE Trans. Magn.*, vol. 28, no. 5, pp. 2196–2198, 1992.

[39] J. P. Yonnet, “Permanent magnet bearings and couplings,” *IEEE Trans. Magn.*, vol. 17, no. 1, pp. 1169–1173, 1981.

$H[kA/m]$	$p_m\ (N.m^{-2})$
630	25200
610	24400
590	23600
570	22800
550	22000
530	21200
510	20400
490	19600
470	18800
450	18000
430	17200
410	16400
390	15600
370	14800
350	14000
330	13200
310	12400
290	11600
270	10800
250	10000
230	9200
210	8400
190	7600
170	6800
150	6000
130	5200
110	4400
90	3600
70	2800
50	2000

TABLE II

H, MODULUS OF THE MAGNETIC FIELD (kA/m); p_m, MAGNETIC PRESSURE $(N.m^{-2})$; $M_s = 32kA/m$

Fig. 1. Arc-shaped permanent magnet whose polarization is radial: the inner curved surface is charged with the magnetic pole surface density $+\sigma^*$ and the outer curved surface is charged with the magnetic pole surface density $-\sigma^*$, the inner radius is r_{in}, the outer one is r_{out}.

Fig. 2. Arc-shaped permanent magnet whose polarization is axial: the upper surface is charged with the magnetic pole surface density $+\sigma^*$ and the lower surface is charged with the magnetic pole surface density $-\sigma^*$, the inner radius is r_{in}, the outer one is r_{out}.

Fig. 3. Device structure: three outer rings (permanent magnet or non-magnetic) radially centered with an inner non-magnetic piston and ferrofluid seals in the air gap between the rings and the piston. $r_{in} = 25mm$, $r_{out} = 28mm$.

Fig. 4. Right: upper and lower non-magnetic rings, a middle ring permanent magnet axially magnetized. Left: magnetic pressure in front of the rings. Bottom: magnetic field radial component at a 0.1 mm distance from the rings, along the Z axis.

Fig. 5. Right: upper and lower non-magnetic rings, a middle ring permanent magnet radially magnetized. Left: magnetic pressure in front of the rings. Bottom: magnetic field radial component at a 0.1 mm distance from the rings, along the Z axis.

Fig. 6. Right: Two ring permanent magnets with opposed axial magnetization. Left: magnetic pressure in front of the rings. Bottom: magnetic field radial component at a 0.1 mm distance from the rings, along the Z axis.

Fig. 7. Right: Two ring permanent magnets with opposed radial magnetization. Left: magnetic pressure in front of the rings. Bottom: magnetic field radial component at a 0.1 mm distance from the rings, along the Z axis.

Fig. 8. Right: axially magnetized upper and lower rings, radially magnetized middle ring. Left: magnetic pressure in front of the rings. Bottom: magnetic field radial component at a 0.1 mm distance from the rings, along the Z axis.

Fig. 9. Right: radially magnetized upper and lower rings, axially magnetized middle ring. Left: magnetic pressure in front of the rings. Bottom: magnetic field radial component at a 0.1 mm distance from the rings, along the Z axis.

Fig. 10. Right: axially magnetized upper and lower rings, radially magnetized middle ring, each axial magnet is half as small as the radial one. Left: magnetic pressure in front of the rings. Bottom: magnetic field radial component at a 0.1 mm distance from the rings, along the Z axis.

Fig. 11. Right: axially magnetized upper and lower rings, radially magnetized middle ring, each axial magnet is twice as high as the radial one. Left: magnetic pressure in front of the rings. Bottom: magnetic field radial component at a 0.1 mm distance from the rings, along the Z axis.